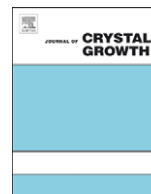




ELSEVIER

Contents lists available at ScienceDirect

Journal of Crystal Growth

journal homepage: www.elsevier.com/locate/jcrysgr

Solar-blind 4.55 eV band gap $\text{Mg}_{0.55}\text{Zn}_{0.45}\text{O}$ components fabricated using quasi-homo buffers

Z.L. Liu^a, Z.X. Mei^a, T.C. Zhang^a, Y.P. Liu^a, Y. Guo^a, X.L. Du^{a,*}, A. Hallen^b, J.J. Zhu^c, A.Yu. Kuznetsov^{c,*}

^a Beijing National Laboratory for Condensed Matter Physics, Institute of Physics, Chinese Academy of Sciences, Beijing 100190, China

^b Department of Microelectronics and IT, Laboratory of Material and Semiconductor Physics, Royal Institute of Technology, Box Electrum 226, SE-164 40 Kista, Sweden

^c Department of Physics, University of Oslo, P.O. Box 1048 Blindern, NO-0316 Oslo, Norway

ARTICLE INFO

Article history:

Received 2 July 2009

Accepted 24 July 2009

Communicated by H. Asahi

Available online 30 July 2009

PACS:

81.15.Hi

81.05.Dz

68.55.ag

78.66.Hf

Keywords:

A1. Phase separation

A1. Solar-blind

A3. Molecular beam epitaxy

B1. MgZnO

B2. ZnO

ABSTRACT

A route for synthesizing high Mg content single-phase wurtzite MgZnO films having band gaps in the solar-blind region is demonstrated by employing molecular beam epitaxy on Al_2O_3 substrates. Importantly, a low Mg content “quasi-homo” buffer, $\text{Mg}_{0.17}\text{Zn}_{0.83}\text{O}$, was applied to accommodate a host of structural discrepancies and therefore, avoiding phase separation in a high Mg content film, $\text{Mg}_{0.55}\text{Zn}_{0.45}\text{O}$, as proved by X-ray diffraction. The Mg fraction in the overgrown single-phase epilayer, $\text{Mg}_{0.55}\text{Zn}_{0.45}\text{O}$, was confirmed by Rutherford backscattering spectrometry.

© 2009 Elsevier B.V. All rights reserved.

1. Introduction

An increasing interest to studies of semiconductor ZnO may be, at least in part, explained by a combination of ZnO superior optical properties—in the first place its large exciton binding energy (~ 60 meV) and wide direct band gap [1]. Moreover, alloying wurtzite ZnO (W-ZnO) with rock-salt MgO (RS-MgO) provides a possibility of band gap tuning in $\text{Mg}_x\text{Zn}_{1-x}\text{O}$ from that of pure W-ZnO (~ 3.4 eV) to that of pure RS-MgO (~ 7.8 eV). Thus, $\text{Mg}_x\text{Zn}_{1-x}\text{O}$ films with tunable band gaps are promising applied as active components in ultra-violet (UV) light emitters [2], solar-blind UV detectors, as well as in other optoelectronic UV-range devices that rely on heterostructure functionalities [3]. Specifically, solar-blind UV detectors, i.e. those dedicated detecting only photons having energies > 4.4 eV, can be used for example for a flame detection, biological/chemical analysis, optical communications within ozone layer, etc [4]. For these applications, it is essential to master manufacturing of single-

phase $\text{Mg}_x\text{Zn}_{1-x}\text{O}$ alloys having band gaps in the solar-blind region.

Already a brief consideration of the equilibrium ternary phase diagram of MgZnO alloy [5,6] suggests that single-phase crystalline alloys may be synthesized only using a limited range of Mg content independently of crystallization lattice—hexagonal wurtzite or cubic rock-salt. Nevertheless and partly because of the application motivations, a significant effort has been devoted to the synthesis of metastable wurtzite (and rock-salt) MgZnO having high Mg contents. Recently, the Mg content in rock-salt MgZnO (RS-MgZnO) was reported to be extended to $\sim 50\%$ reaching a cut-off response wavelength of 287 nm [7]. However, a relatively low photo-response and structural discrepancy from that of ZnO may limit the application of the results obtained in Ref. [7]. On the other hand wurtzite MgZnO (W-MgZnO), accounting for its promising optical properties [8] and the same structure as that of ZnO, remains an interesting and important material to be investigated. Thus, it is essential to develop reproducible synthesis routes for single-phase W-MgZnO with a band gap larger than 4.4 eV. The challenge is avoiding so-called phase separation in MgZnO which is due to a significant structural difference between wurtzite and rock-salt structures of the alloy components. Moreover, theoretical studies have shown that wurtzite MgO (W-MgO) has an unusual 5-fold coordinated

* Corresponding authors. Tel.: +86 10 82649035; fax: +86 10 82649228.

E-mail addresses: xldu@aphy.iphy.ac.cn (X.L. Du), andrej.kuznetsov@fys.uio.no (A.Yu. Kuznetsov).

structure induced by strong ionicity of Mg–O bonds [9], which is quite different from that 4-fold W-ZnO explaining that the phase separation is an issue even if considering that both components having a wurtzite structure. However, the influence of the strong ionicity of Mg–O bond on the structural distortion induced into the W-ZnO matrix during synthesis of W-MgZnO alloys was practically ignored in most of the previous experimental studies. Anyhow, addressing the issues several types of buffer layers with hexagonal surface structures, specifically RS-MgO (111) and W-ZnO (0001), were used for growing MgZnO films epitaxially on c-sapphire substrate [10,11]. For example, single-phase W-MgZnO with a band gap of 3.99 eV was prepared by pulsed laser deposition [12], and a $\text{Mg}_{0.44}\text{Zn}_{0.56}\text{O}$ film with a band gap of 4.25 eV was demonstrated using ZnO buffer layer by molecular beam epitaxy (MBE) [13]. Note, the synthesis of MgZnO with high Mg fractions used to suffer from severe reproducibility problems as often honestly emphasized by the authors [14]. In this letter, we report on a realization of single-phase high Mg content W-MgZnO thin films with a band gap in the solar-blind region that were synthesized employing a “quasi-homo” MgZnO buffers having a low Mg content (typically $\text{Mg}_{0.17}\text{Zn}_{0.83}\text{O}$ as determined in the course of the work). Comparing to either ZnO or MgO buffers the $\text{Mg}_{0.17}\text{Zn}_{0.83}\text{O}$ quasi-homo buffer provides better conditions for accommodating structural differences between binary components when growing high Mg content MgZnO films.

2. Experimental

The samples were synthesized on sapphire (0001) substrates by rf-plasma assisted MBE with a base pressure of $\sim 1 \times 10^{-10}$ mbar. Elemental Mg (5N) and Zn (7N) evaporated by Knudsen cells (CreaTech) and radical oxygen generated by rf-plasma system (SVTA) were used as sources for the growth. Before loading into the growth chamber, the substrates were firstly degreased in hot acetone followed by rinsing in alcohol and, subsequently, in deionized water. After loading into the chamber the substrates were heated up to 750 °C for thermal cleaning and subsequently exposed for oxygen plasma “pre-treatment” at 250 °C in order to obtain a uniform oxygen-terminated surface [15]. The synthesis of both quasi-homo buffers (~ 20 nm) and high Mg content epilayers (~ 200 nm) were performed at 450 °C keeping the pressure at 4.5×10^{-5} mbar and Zn-cell temperature at 311 °C. After depositing low Mg content buffers, three samples (labeled as A0, A, and A1) were fabricated using Mg fluxes of 1.3×10^{14} , 1.4×10^{14} and 1.6×10^{14} atoms/cm²s, respectively. Additionally, a set of MgZnO samples grown directly on sapphire substrates without buffers were prepared and used for comparison. Specifically, one of such samples expected having an intermediate Mg content is labeled as sample B. Crystallographic properties of the samples were studied by reflection high-energy electron diffraction (RHEED), X-ray diffraction (XRD) and high-resolution X-ray diffraction (HRXRD) using light source from synchrotron radiation. The Mg content in MgZnO films was estimated from XRD measurements and confirmed by Rutherford backscattering spectrometry (RBS) employing 2 MeV He⁺ ions and SIMRA code for fitting the experimental and simulation data. Optical band gaps in the samples were further investigated using a combination of transmittance and reflectance measurements which were performed on a commercial spectrophotometer system (LAMBDA 950, PERKIN ELMER) at room temperature. The light sources were 150W deuterium and halogen lamps from which a parallel and small angle (8°) beam to the normal of the sample were employed for transmittance and reflectance tests, respectively.

3. Results and discussion

3.1. Structural characterization

Fig. 1 shows RHEED patterns of sample A before and after MgZnO growth. Fig. 1(a) is taken from the substrate surface right after the oxygen radicals pre-treatment and the sharpness of the patterns indicates a clean and flat surface before starting the deposition. The growth of a low Mg-content MgZnO buffer layer (to be used as a quasi-homo template later on) results in a well-defined single wurtzite phase structure as confirmed by the 6-fold symmetry of the RHEED pattern (see Fig. 1(b)). In addition, relatively streaky RHEED patterns indicate a reasonable flatness of the buffer. Further, a single-phase wurtzite structure is observed in the nominally higher Mg content MgZnO films (see Fig. 1(c)) overgrown on the quasi-homo buffer prepared in the previous step, Fig. 1(b). The contrast and the shape of the RHEED patterns in Fig. 1(c) reveal a smooth surface and the 6-fold symmetry of a single wurtzite phase.

XRD θ – 2θ scans were measured on all samples to study eventual phase separation and Fig. 2 illustrates the results obtained from samples A, A0, A1 and B. Firstly, Fig. 2(c) shows the results obtained from sample A containing a high Mg content film overgrown on a low Mg content buffer. There are two peaks at 34.91° and 41.68° found corresponding to W-MgZnO (002) and sapphire (006) planes, respectively. No other significantly strong signals related to other phases, e.g. rock-salt (111) at 36.9° or rock-salt (200) at 42.9° are detected suggesting that no phase separation and emerging of RS-MgO occurs in the overgrown MgZnO film. A slight asymmetry in the W-MgZnO (002) peak can

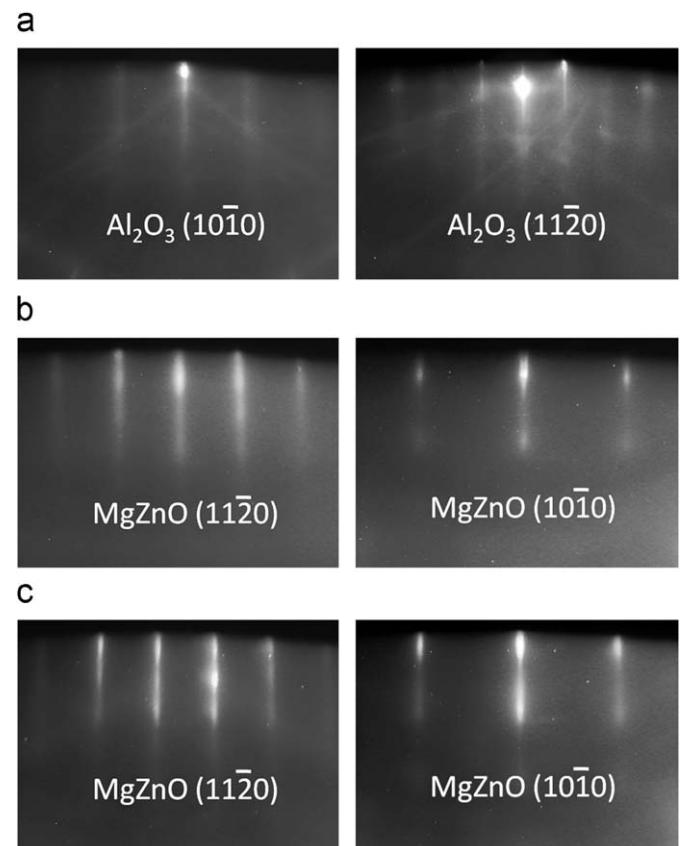


Fig. 1. RHEED patterns along two fixed electron azimuths as measured after different steps of the sample A fabrication: (a) sapphire substrate oxygen plasma pre-treatment, (b) low Mg content quasi-homo buffer synthesis, and (c) MgZnO epitaxy.

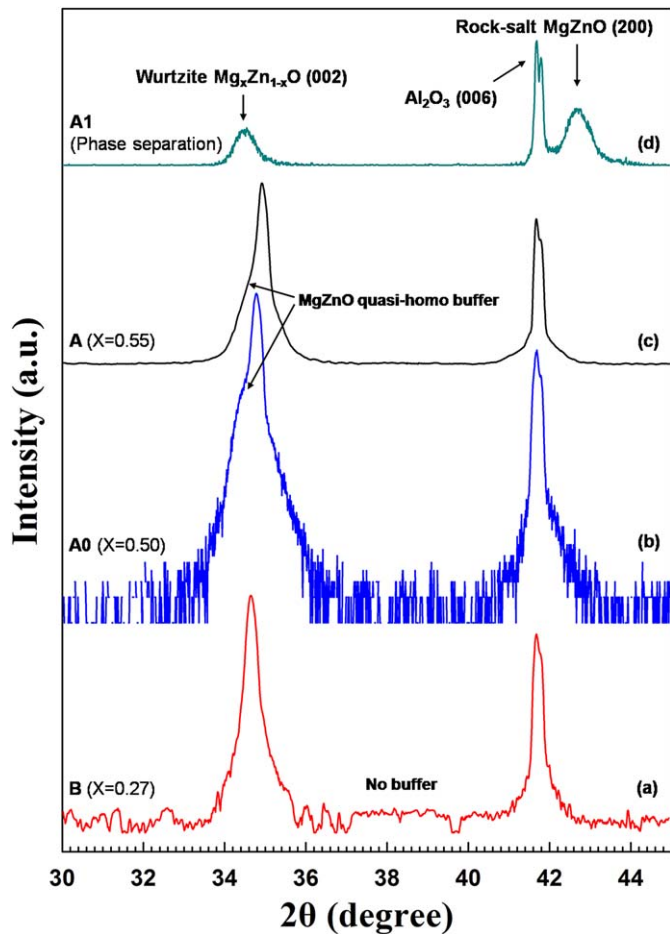


Fig. 2. X-ray diffraction θ – 2θ scans of samples A, A0, A1 and B. Note, the XRD intensity is plotted using a logarithmic scale.

be explained by the contribution from the low Mg-content buffer underneath. Furthermore, the W-MgZnO (002) peak shifts to significantly larger angles comparing to that for pure ZnO (002) – typically detected at $\sim 34.46^\circ$ – suggesting that the c lattice parameter in the W-MgZnO decreases with increasing Mg content relative to that of ZnO [12]. In its turn, the magnitude of the shift observed in Fig. 2(c) implies a Mg fraction of 55% incorporated into the epilayer of sample A (also confirmed by RBS as going to be discussed later). Importantly, our synthesis of single-phase W-MgZnO with a Mg content up to 55% is reproducible and controllable as long as the Mg flux is less than a critical value which is illustrated in Fig. 2(b) and (d). Indeed, a similar asymmetric peak attributed to W-MgZnO (002) was found in sample A0 which was grown using $\sim 7\%$ smaller Mg flux than that in sample A resulting in a corresponding decrease of Mg content down to 50%, Fig. 2(b). In contrast, increasing the Mg flux by $\sim 15\%$ in sample A1 results in a wurtzite/rock-salt phase separation in MgZnO as shown in Fig. 2(d). The phase separation was also confirmed by in-situ RHEED observations during the fabrication of sample A1—a new set of RHEED patterns (not shown) corresponding to RS-MgZnO emerge upon the epilayer synthesis. On the other hand, the growth of MgZnO films directly on sapphire substrate without low Mg content buffers is characterized by an appearance of a symmetric W-MgZnO peak as illustrated in Fig. 2(a) for sample B. However, our systematic study reveals that the phase separation in samples synthesized on the substrate readily occurs for Mg fractions $\geq 45\%$. Thus, our quasi-homo buffer approach extends the limits of Mg incorporation into W-MgZnO by at least 10%.

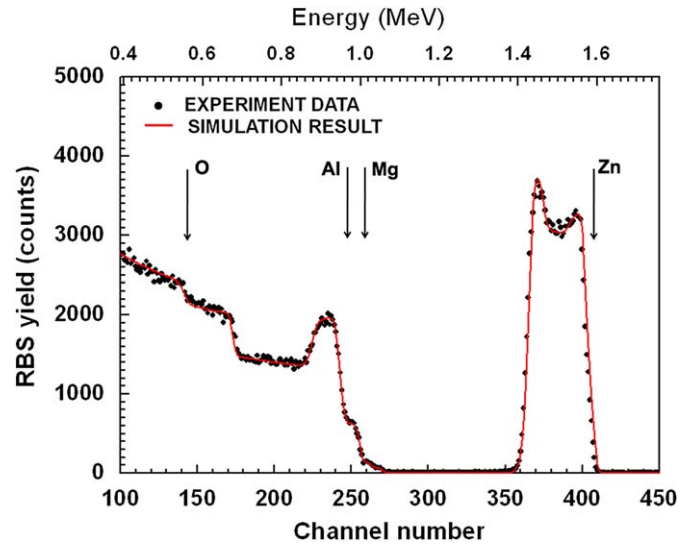


Fig. 3. RBS spectrum taken from sample A (points) and a corresponding best-fit simulating a $\text{Mg}_{0.55}\text{Zn}_{0.45}\text{O}/\text{Mg}_{0.17}\text{Zn}_{0.83}\text{O}/\text{Al}_2\text{O}_3$ structure (line).

3.2. RBS characterization

Further, Fig. 3 shows an RBS spectrum taken from sample A. Arrows/labels in Fig. 3 indicate the channel number at which the backscattering from the corresponding elements starts. Note that the signals from Mg and Al are partly overlapping. The fitting of the experimental and simulation data in Fig. 3 reveals the composition of the sample— $\text{Al}_2\text{O}_3/20\text{ nmMg}_{0.17}\text{Zn}_{0.83}\text{O}/200\text{ nmMg}_{0.55}\text{Zn}_{0.45}\text{O}$, consistently with the XRD results. The incorporation of 55% Mg into MgZnO without phase separation is, in our view, a sensational result and more studies have to be performed investigating mechanisms of phase stabilization of W-MgZnO in our samples. In addition, the composition of the intermediate Mg-content sample – sample B – was determined by RBS as $\text{Al}_2\text{O}_3/200\text{ nmMg}_{0.27}\text{Zn}_{0.73}\text{O}$.

3.3. Optical characterizations

Room-temperature transmittance spectra of the samples containing the intermediate (sample B) and high Mg contents (sample A) are shown in Fig. 4. Two absorption edges at ~ 270 and $\sim 340\text{ nm}$ are revealed in sample A, which are attributed to the $\text{Mg}_{0.55}\text{Zn}_{0.45}\text{O}$ epilayer and the $\text{Mg}_{0.17}\text{Zn}_{0.83}\text{O}$ buffer, respectively. A relatively “flat” absorption edge associated with the $\text{Mg}_{0.17}\text{Zn}_{0.83}\text{O}$ buffer can be explained in terms of significant fluctuations in Mg content and high density of defects through the buffer. On the other hand the “as-grown” $\text{Mg}_{0.17}\text{Zn}_{0.83}\text{O}$ buffer shows a good structural quality (Fig. 1(b)) and rather sharp absorption cut-offs (not shown but the shapes are readily comparable with that for $\text{Mg}_{0.27}\text{Zn}_{0.73}\text{O}$ in Fig. 4). A possible hypothesis explaining different properties of “own-standing” and “overgrown” buffers is that, when overgrown, the buffer accommodates a host of structural discrepancies between ZnO and MgO enabling the formation of metastable single-phase W-MgZnO alloy at a cost of a dramatic degradation happening, fortunately, in the buffer only. Indeed, the absorption edge at 270 nm in $\text{Mg}_{0.55}\text{Zn}_{0.45}\text{O}$ is nearly as sharp as that of $\text{Mg}_{0.27}\text{Zn}_{0.73}\text{O}$ indicating negligible fluctuations of Mg composition, high crystalline quality, and suggesting our single-phase wurtzite $\text{Mg}_{0.55}\text{Zn}_{0.45}\text{O}$ film to be a suitable component for the fabrication of solar-blind UV detectors. Note that our method of

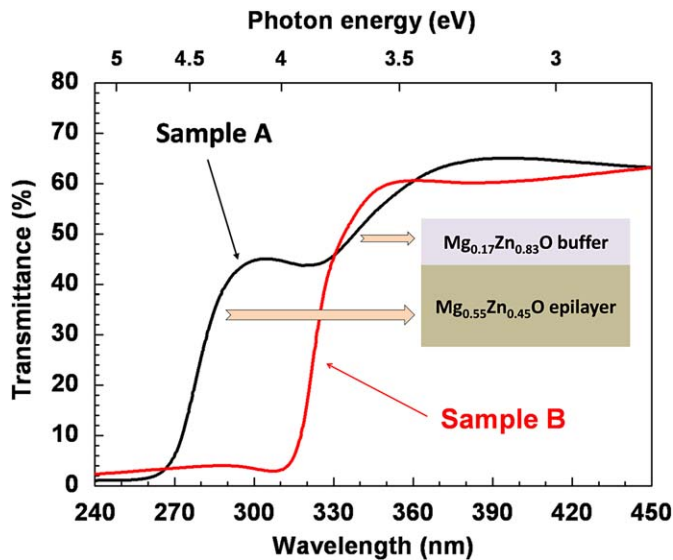


Fig. 4. Room temperature transmittance spectra of samples A (black line) and B (red line). (For interpretation of the references to colour in this figure legend, the reader is referred to the web version of this article.)

MgZnO overgrowth of quasi-homo buffers demonstrates a good reproducibility in a series of experiments.

Large exciton binding energy – well known for ZnO-related materials including MgZnO ternary alloys – complicates the determination of the band gap. For example, because of the strong excitonic nature, linear fitting employing the relationship of $\alpha^2 \propto (E - E_g)$ is not satisfactory for acceptable estimation of the band gap of MgZnO (α is an absorption coefficient). In the present work, the band gaps were calculated based on the data in Fig. 4 in combination with reflectance spectrometry by using differential absorption coefficient versus photon energy, in which Urbach tail and Elliott's formula were employed to describe the inner-bandgap and inter-band transition [16–18]. Additionally, excitonic transition peaks [13] can be observed in the high-energy side of the reflection spectra of both samples A and B with transition energy of 4.55 and 3.92 eV, respectively. Finally, the band gap in our $\text{Mg}_{0.55}\text{Zn}_{0.45}\text{O}$ was found to be as high as 4.55 eV well entering into the solar-blind UV region.

4. Conclusions

In summary, we have successfully synthesized single-phase wurtzite $\text{Mg}_{0.55}\text{Zn}_{0.45}\text{O}$ thin films on quasi-homo $\text{Mg}_{0.17}\text{Zn}_{0.83}\text{O}$

buffers by rf-plasma assisted MBE. The MgZnO buffer is found playing a key role in the non-equilibrium growth dynamics providing functions of (i) a wurtzite template for accommodating the high Mg-content wurtzite epilayer and (ii) a relaxation space for the lattice distortions induced by strong ionic Mg–O bonds. Furthermore, the reproducibility of such metastable synthesis was confirmed in series of the experiments. Finally, having a band gap of 4.55 eV $\text{Mg}_{0.55}\text{Zn}_{0.45}\text{O}$ films are suggested to be suitable components for fabricating solar-blind UV detectors.

Acknowledgments

This work was supported by the National Science Foundation (Grant nos. 50532090, 60606023, 60621091, 10804126) and the Ministry of Science and Technology (Grant nos. 2007CB936203, 2009CB929400) of China as well as by the Research Council of Norway through the FRINAT “Understanding ZnO” project.

References

- [1] D.M. Bagnall, Y.F. Chen, Z. Zhu, T. Yao, M.Y. Shen, T. Goto, Appl. Phys. Lett. 73 (1998) 1038.
- [2] A. Ohtomo, M. Kawasaki, I. Ohkubo, H. Koinuma, T. Yasuda, Y. Segawa, Appl. Phys. Lett. 75 (1999) 980.
- [3] A. Tsukazaki, A. Ohtomo, T. Kita, Y. Ohno, H. Ohno, M. Kawasaki, Science 315 (2007) 1388.
- [4] E. Monroy, F. Omnès, F. Calle, Semicond. Sci. Technol. 18 (2003) R33–R51.
- [5] W. Yang, S.S. Hullavarad, B. Nagaraj, I. Takeuchi, R.P. Sharma, T. Venkatesan, R.D. Vispute, H. Shen, Appl. Phys. Lett. 82 (2003) 3424.
- [6] S. Choopun, R.D. Vispute, W. Yang, R.P. Sharma, T. Venkatesan, H. Shen, Appl. Phys. Lett. 80 (2002) 1529.
- [7] Z.G. Ju, C.X. Shan, D.Y. Jiang, J.Y. Zhang, B. Yao, D.X. Zhao, D.Z. Shen, X.W. Fan, Appl. Phys. Lett. 93 (2008) 173505.
- [8] H. Shibata, H. Tampo, K. Matsubara, A. Yamada, K. Sakurai, S. Ishizuka, S. Niki, M. Sakai, Appl. Phys. Lett. 90 (2007) 124104.
- [9] W. Lambrecht, S. Limpijumnong, B. Segall, MRS Internet J. Nitride Semicond. Res. 4S1 (1999) G6.8.
- [10] Z. Vashaei, T. Minegishi, T. Yao, J. Cryst. Growth 306 (2007) 269/275.
- [11] Z. Vashaei, T. Minegishi, H. Suzuki, T. Hanada, M.W. Cho, T. Yao, A. Setiawan, J. Appl. Phys. 98 (2005) 054911.
- [12] A. Ohtomo, M. Kawasaki, T. Koida, K. Masubuchi, H. Koinuma, Y. Sakurai, Y. Yoshida, T. Yasuda, Y. Segawa, Appl. Phys. Lett. 72 (1998) 2466.
- [13] H. Tampo, H. Shibata, K. Maejima, A. Yamada, K. Matsubara, P. Fons, S. Niki, T. Tainaka, Y. Chiba, H. Kanie, Appl. Phys. Lett. 91 (2007) 261907.
- [14] T. Takagi, H. Tanaka, S. Fujita, S. Fujita, Jpn. J. Appl. Phys. 42 (2003) L401.
- [15] Z.X. Mei, Y. Wang, X.L. Du, M.J. Ying, Z.Q. Zeng, H. Zheng, J.F. Jia, Q.K. Xue, Z. Zhang, J. Appl. Phys. 96 (2004) 7108.
- [16] F.A. Ponce, S. Srinivasan, A. Bell, L. Geng, R. Liu, M. Stevens, J. Cai, H. Omiya, H. Marui, S. Tanaka, Phys. Status Solidi (b) 240 (2) (2003) 273–284.
- [17] F. Urbach, Phys. Rev. 92 (1953) 1324.
- [18] R.J. Elliott, Phys. Rev. 108 (1957) 1384.